Proc. Lunar Planet. Sci. Conf. 11th (1980), p. 2447–2462
Printed in the United States of America

Ridge systems of Caloris: Comparison with lunar basins

Ted A. Maxwell and Ann W. Gifford

Center for Earth and Planetary Studies, National Air and Space Museum, Smithsonian Institution, Washington, D.C. 20560

Abstract—Ridges within the Caloris basin on Mercury display several of the traits that are characteristic of mare-type ridges in multi-ring basins on the moon. Among these similarities are the predominance of basin-concentric and radial orientations, and the location of ridges inside topographic benches at the edge of the basin. The ratio of the most prominent ridge-ring diameter to basin rim diameter for Caloris is consistent with that of lunar multi-ring basins. However, if it is assumed that the major circumferential ridge systems formed directly over peak rings, then there does not seem to be a simple progression in the diameter of peak rings from unfilled lunar basins to multi-ring basins.

Based on comparable measurements of Caloris and the eastern portions of lunar multi-ring basins, both the orientation and frequency of ridges in lunar basins indicate the effect of global-scale, east-west compression. In the northern and southern sectors of lunar basins, globally induced stress dominated over that produced by basin downdropping, and caused ridge systems to deviate into the highlands, perhaps controlled by older fracture systems. In contrast to the ridge systems of lunar multi-ring basins, the strong basin-related trends within Caloris support previous studies that have suggested a post contraction/despinning(?) time of formation for structural features within the Caloris basin.

INTRODUCTION

The wrinkle ridge systems of the Caloris basin on Mercury display many of the traits that are characteristic of ridges in the mare-filled lunar multi-ring basins. Because of limitations of Mariner 10 image resolution, it is unknown whether small-scale features such as the crenulated crests and the dominant "ropy" type of morphology associated with lunar mare ridges are present within Caloris. Nonetheless, the broad, arch-like appearance, concentric and radial orientations, and predominant localization within the main ring of the Caloris basin suggest that these features are analogous to lunar mare ridges and arches. Among the several hypotheses that have been advanced to explain the origin of lunar mare ridges, a tectonic mode of formation has been preferred on the basis of several previous studies (Muehlberger, 1974; Maxwell *et al.*, 1975; Lucchitta, 1976, 1977; Maxwell, 1978). Assuming an origin by horizontal compression, Solomon and Head (1980) used the placement of mare ridges in lunar basins in order to model thickness variations of the elastic lunar lithosphere. Consequently, although the details of mare ridge formation are still not well known, the use of these features for tectonic models necessitates further study of their distribution and probable

origin. In this study, we will concentrate on the ridge systems within the Caloris basin on Mercury, and implications for the origin of ridges within basins on both Mercury and the moon.

Previous studies of ridges and scarps on Mercury have been done primarily on a global scale, although several details of the Caloris ridges have not been overlooked. Strom *et al.* (1975) noted that ridges occur on both the hummocky and smooth plains surrounding Caloris, and that within Caloris, they are best developed in a zone 170 km wide, centered 120 to 140 km from the edge of the basin. Subsidence of the interior of Caloris was thought to be responsible for generating the compressive stress needed for ridge formation, although uplift and fracture of the central part of the basin may have occurred at a later time (Strom *et al.*, 1975). In an extensive study of ridges and scarps on Mercury, Dzurisin (1978) suggested that subsidence of Caloris may have been due to magma withdrawal from beneath the basin to form the later-emplaced smooth plains surrounding Caloris. Continuing isostatic adjustment to basin excavation was thought to be responsible for later uplift and the extensional fractures of the central part of the basin (Dzurisin, 1978).

The results of previous studies of mercurian scarps (Strom *et al.*, 1975; Cordell and Strom, 1977; Melosh and Dzurisin, 1978a; Dzurisin, 1978) all suggest that the tectonic features of the Caloris basin were formed *after* or during the waning stages of global thermal contraction or tidal despinning. Consequently, ridges and other tectonic features within Caloris should be primarily the result of basin-induced stress with a relatively minor component of a global stress field. Therefore, the purpose of this study is to compare the distribution and orientations of ridges within the Caloris basin to those of lunar basins in an attempt to provide photogeologic evidence for the relative effects of global versus basin-induced stress on both the Moon and Mercury.

RIDGE SYSTEMS OF THE CALORIS BASIN

Although broadly similar to the placement of ridges within lunar mare-filled basins, ridges in Caloris are more widely distributed than their lunar counterparts. Based on the 1:5,000,000 shaded relief map of the Caloris Planitia Area of Mercury (USGS, 1979), the main ring of the Caloris basin consists of a broken arc describing a basin diameter of 1420 km (centered at 30°N, 197°W; 40 km west of the center of the map projection used in Caloris map sheet). The main ring of ridges (inner-ring ridge system) occurs at a diameter of 1060 km (Fig. 1). In addition, a subtle ring in the central part of the basin (approximately 800 km in diameter) is represented by a highly-fractured, gentle topographic rise approximately 30 km wide.

The major morphological difference between ridges of Caloris and their lunar counterparts is that the narrow, sinuous ridges that occur on the crests of lunar mare arches appear to be absent on the structures within Caloris (Strom *et al.*, 1975). However, as pointed out by Malin (1978), the resolution of earth-based photographs of the moon is the most comparable to that of Mariner 10 images of

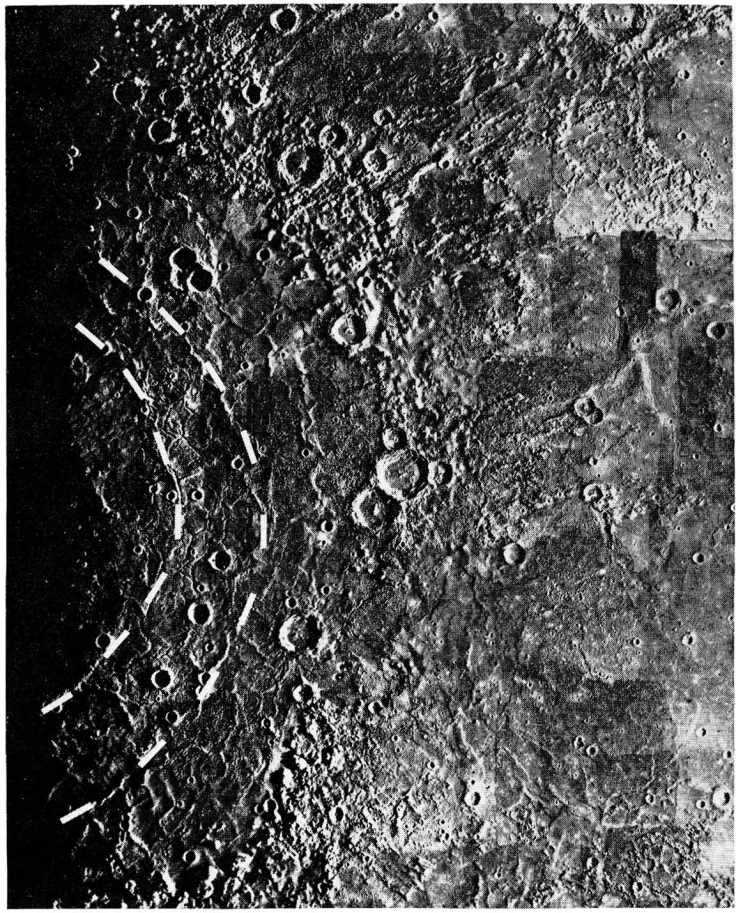

Fig. 1. Photomosaic of the Caloris Basin. Two inner-basin rings are indicated; innermost ring is composed of a gentle topographic arch 800 km in diameter. Prominent ring of ridges (second ring) is 1060 km in diameter.

Mercury. Examination of ridge systems on photographs from Kuiper *et al.* (1967) reveals that the narrow crestal ridges documented on Lunar Orbiter images and Apollo photographs appear severely degraded, but can still be recognized on properly oriented, sun-facing portions of the ridge. Similar narrow ridges are present in parts of the Caloris basin interior, where they generally follow the same orientations as the underlying arch although they deviate from side to side. Because of the varying resolution of Mariner 10 images, it is not possible to estimate the abundance of the smaller ridges within Caloris, but their existence in a few locations supports the analogy with lunar mare ridges.

In contrast to the occurrence of lunar mare ridges in single rings, the multiple concentric ridges of Caloris occur in a broad zone just within the main rim of the basin (Strom *et al.*, 1975; Dzurisin, 1978). They extend from a diameter of 1000

km to 1320 km (Fig. 2), and are accompanied by abundant fractures to a diameter range of 1300 km. The observation that these fractures crosscut the ridges led Strom *et al.* (1975) and Dzurisin (1978) to hypothesize later updoming of the center of the basin. Since no similar fractures are present in the central portions of lunar basins, it is possible that Caloris experienced a late-stage tectonic episode very different from the evolutionary trend of lunar basins. Nonetheless, an early episode of basin subsidence, consistent with the gross topography derived from isophotes (Hapke *et al.*, 1975), may have formed the Caloris ridges in a manner similar to that hypothesized for lunar ridges.

On the moon, the association of ridges with changes in mare level (Lucchitta,

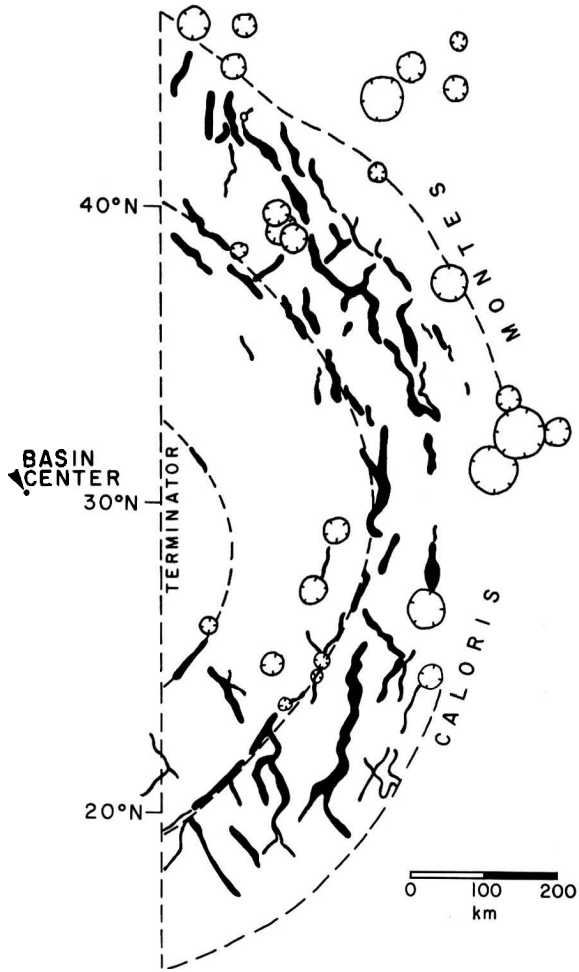

Fig. 2. Sketch map showing distribution and orientation of lunar-like wrinkle ridges within the Caloris Basin. Ridges are located predominantly between the second and third rings of the basin.

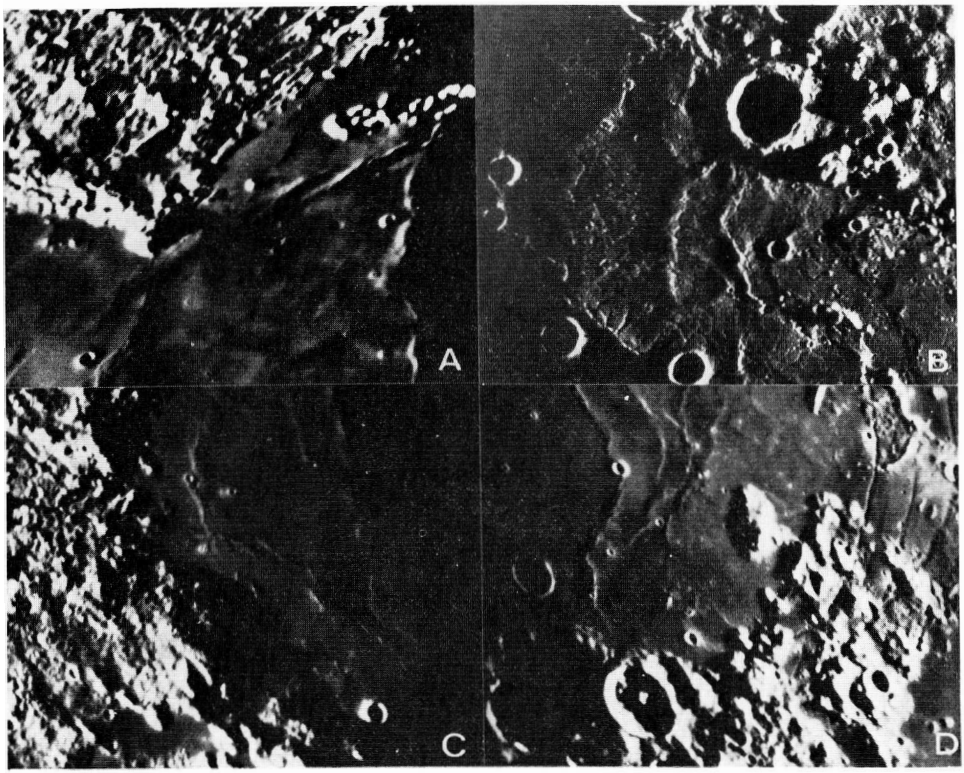

Fig. 3. Topographic benches and associated ridges in lunar basins (from earth-based photos) and Caloris (Mariner 10). A) Northwest Imbrium; Sinus Iridum (left side of picture) is topographically higher than central Mare Imbrium. B) Caloris; note bench (letter "B"), and graben-like trough similar to that of the Sulpicius Gallus region in southwestern Mare Serenitatis (C). D) Southeastern quadrant of the Humorum Basin; note basin-concentric systems of rilles and ridges and 80 km wide bench region.

1977), the edges of surface disc mascon models (Phillips *et al.*, 1972) and topographic benches surrounding the mascon basins all support an origin related to subsidence of the inner basin. Additional evidence for offsetting of subsurface mare contacts and probable normal faulting in Mare Crisium (Maxwell and Phillips, 1978), and subsidence of the inner part of Mare Serenitatis (Peeples *et al.*, 1978) indicates that downdropping took place before the latest period of mare basalt emplacement. Within Caloris, lunar-like topographic benches occur on both the northeastern and southeastern portions of the basin rim. In northeastern Caloris, a 70 km wide bench extends for 250 km along the arc of the basin, and is separated from the inner part of the basin by an upraised lip of small, discontinuous mare ridges (Fig. 3). A similar bench is present in southeastern Caloris, but here is only 30 km wide. Apparently, the later uplift of the central basin did not affect the bench regions, since the fractures occur basinward of the scarps.

As shown above, the morphology, basin-related setting and probable structural

relationships with the benches in Caloris are similar to the setting of ridge systems of lunar mare basins. However, the use of Caloris ridges as an example of basin-induced stress is strongly dependent on the interpretation that these features formed after the period of mercurian global compression. Evidence for their relatively late-stage formation is based on both the global density of lobate scarps, and the relative age of the Caloris-related smooth plains. Cordell and Strom (1977) found that relatively few lobate scarps were found in the latitudes occupied by hilly and lineated terrain, which implied that any scarps that may have existed were destroyed at the time of the Caloris impact. They also noted, however, that several scarps are present on the post-Caloris smooth plains. Dzurisin (1978) also supported a post-contraction/despinning time of origin for Caloris, and attributed the scarps in the smooth plains surrounding Caloris to local gravitational adjustments. Separating the mercurian global lineaments from the arcuate scarps, Melosh and Dzurisin (1978a) found that very few lineaments and no arcuate scarps are present in the area affected by Caloris, and thus concluded that the Caloris basin formed after contraction ceased.

Additional evidence for the late-stage formation of Caloris-related structures is based on the time of emplacement of the Caloris smooth plains. Wood *et al.* (1977) noted that the smooth plains were emplaced after the beginning of the time of formation of Class 1 craters (LPL Classification; fresh craters). Thus, the material that is deformed by the ridges most likely was not present until well after the end of heavy bombardment.

In spite of these stratigraphic arguments for the formation of Caloris-related structures after global compression, it is still possible that the global lineament system may have affected the distribution and orientation of Caloris ridges. In addition to this possible inheritance factor, both Solomon (1977) and Strom (1979) note that Mercury should have experienced a relatively longer period of global compression than the other terrestrial planets. Consequently, the comparison of Caloris ridges with those of lunar basins should also allow an assessment of the relative importance of pre-basin fracture systems.

COMPARISON OF CALORIS WITH LUNAR BASINS

Comparison of Caloris basin structure with that of lunar basins is limited by three factors: 1) sun azimuth, which may hinder identification of east-west oriented structures; 2) low resolution of Mariner 10 images, when compared to Apollo metric and panoramic camera photographs and Lunar Orbiter images; and 3) images of only one-third of the Caloris basin are available for comparison with the more completely photographed lunar basins.

Due to the sinuous, segmented nature of both lunar and mercurian ridges, sun azimuth does not seem to be an important factor in biasing observations of ridge distribution and orientation. East-west oriented ridges can be seen on both the moon (in southern Mare Serenitatis and southern Mare Imbrium) and Mercury (Fig. 1), which suggests that their absence in other parts of the basins is real

rather than an artifact of lighting. To compensate for the low resolution of Mariner 10 images, only those ridges and arches visible at the resolution of telescopic photographs (Kuiper *et al.*, 1967) were included for comparison with Caloris.

The most important limitation, the incomplete coverage of Caloris, is more difficult to contend with. In order to have a lunar data set comparable to that for Caloris, we have used only the eastern one-third of lunar multi-ring basins in our analysis of the distribution and orientation of ridges. Similar orientation data for entire lunar basins exist elsewhere in the literature (Strom, 1964; Elston *et al.*, 1971; Maxwell *et al.*, 1975; Fagin *et al.*, 1978), although there is no standardization for mapping or weighting procedures.

Ridge orientation

Two methods were used to study the orientation of ridges within Caloris and the lunar mare-filled basins of Crisium, Humorum, Serenitatis, and Nectaris. The orientation of each linear ridge segment was measured with respect to north, weighted according to its length (organized into number of kms of ridge per orientation), and plotted for the entire eastern one-third of the basins studied. In addition, these data were also broken down into 15° sectors, and plotted according

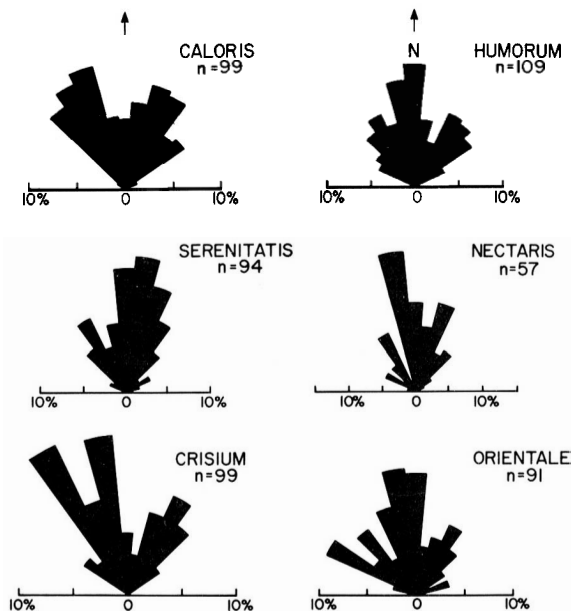

Fig. 4. Orientations of ridges occurring in the eastern one-third of Caloris and four lunar mare-filled basins. Hypothetical ridge orientations for Orientale are based on lineament trends and the few existing mare ridges that are present in the central part of the basin.

to the location of the sector. In order to provide some estimate on the expected subsurface structure within lunar basins, the orientations of lineaments, existing ridges, and areas of protruding topographic relief in the eastern part of the Orientale basin were measured in a manner similar to that used for Caloris and the mare-filled lunar basins. Because it is uncertain whether some of the smaller-scale ridges or lineaments might contribute to hypothetical Orientale ridge systems, these data were not broken down into 15° segments. Nonetheless, the major trends of Orientale are included for comparison with total (one-third) basin orientations.

As shown in the rose diagrams of ridge orientations for the eastern one-third of the basins (Fig. 4), Caloris shows much stronger maxima at N30°E and N30°W than do lunar basins. Although these orientations are consistent with fracture trends predicted by Melosh and Dzurisin (1978a) for a model of early tidal despinning of Mercury, the locations of these prominent trends indicate that they are imposed primarily by the geometry of the basin. In contrast, the orientations in Serenitatis, Humorum, Nectaris, and Orientale show maxima in a general northerly direction, while Crisium is strongly skewed to the northwest.

When plotted according to location within the basin, the reason for the NW and NE enhancement of ridge trends in Caloris is apparent (Fig. 5). The north-

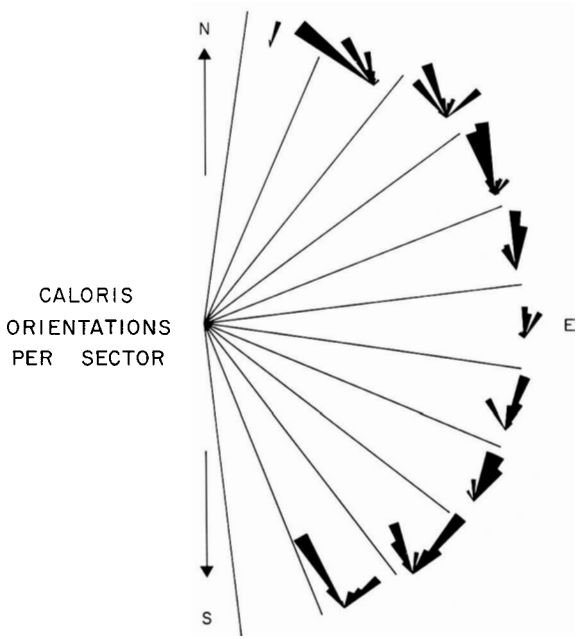

Fig. 5. Ridge azimuths per 15° sector for the Caloris Basin. Length of rose diagram segments are normalized to total length of ridges in each sector. Note the prevalence of basin concentric and radial trends, and weak NS orientations in the eastern sectors of the basin.

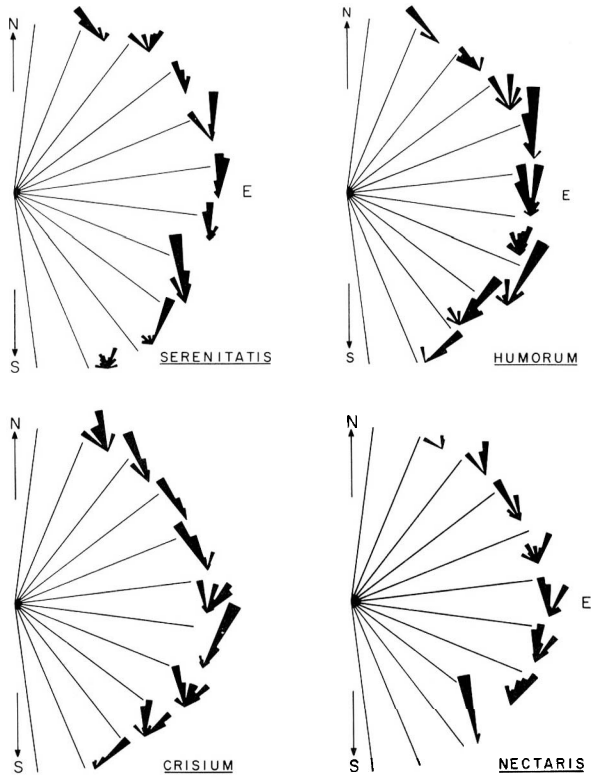

Fig. 6. Ridge azimuths for four lunar mare-filled basins; method of plotting is the same as used for Caloris (Fig. 5). Lunar ridges exhibit much greater variability in orientation than those of Caloris. Strong N-S trends are particularly well-developed in the Serenitatis and Humorum basins.

west trends are most strongly developed in the northeast where they are concentric to the basin, and in the southeast where they are radial to the basin. Similarly, the slightly weaker northeast mode is due to less prominent concentric ridges in the southeast, and radial ridges in the northeast. Both the low number of ridges in the eastern sector and the basinwide lack of north-trending ridges distinguish the Caloris orientation pattern from that of lunar basins (Fig. 6).

The orientations of ridges in the Caloris basin are more strongly concentric than those of either ridges in the flooded lunar basins studied here, or lineaments in the Orientale basin. In Caloris, 61% of all orientations measured are within 20° of being concentric to the center of the basin, and 19% are within 20° of being radial. For comparison with a flooded lunar basin, only 43% of the ridges in the eastern third of Serenitatis are within 20° of being concentric, and 16% are within 20° of being radial. In the relatively pristine Orientale basin, 43% of the lineaments, scarps and ridges are concentric, while 11% of these features form radial trends.

Consequently, the total orientations for the corresponding portions of Caloris and five lunar basins, and the orientations per sector of the basins both suggest that Caloris ridges are more closely related to basin-controlled radial and concentric orientations than are lunar basin ridge systems. On the basis of these data plotted for the entire eastern third of the basins studied here, the closest lunar analog to the Caloris ridge systems would be those of Crisium (Fig. 4). However, when broken down into sectors, it is apparent that the NW and NE modes of Crisium ridges are not created by strong radial components (Fig. 6).

Ridge distribution

A comparable treatment of the geographic distribution of Caloris and lunar basin ridges was done by: 1) comparing the diameter of the most prominent ring of ridges to that of the next outer ring of the basin, and 2) simply counting the number of ridges present along a line radial to the basin, in order to identify areas of maximum stress.

Relation to basin ring structure

Although much controversy surrounds both the mode of origin of lunar basin rings and the meaning of various ratios of ring diameters, the concentric pattern of ridge systems and their extension as highland fractures indicates involvement of the pre-mare surface, which was formed as a result of impact and later basin modification. In fact, the location of the lunar ridge systems has traditionally been used to define the inner-rings of mare-filled basins (Wilhelms and McCauley, 1971). Hartmann and Wood (1971) advocated a genetic relationship between peak rings and wrinkle ridges, although they attributed ridge formation to intrusion and extrusion of mare basalt. Nonetheless, they found a somewhat consistent ratio between the diameter of the prominent circular ridge system and the next largest basin rim (see Table VI in Hartmann and Wood, 1971). Brennan (1976), in a review of basin ring spacings, found no consistent ratio for outer rings, but did find an extremely high correlation between the diameter of the ridge ring and basin rim for five lunar mare-filled basins. Head (1977) believed that the position of the concentric mare ridge system marked the location of the central peak ring (termed "central peak ring" in Head, 1977) in lunar multi-ringed basins, and noted that Imbrium exhibits both the ridge system and numerous peak ring segments.

In order to examine the role of basin ring structure in controlling ridge location in both Caloris and lunar basins, we first extrapolated the best-fit curve of peak ring diameter (Dr, for peak-ring basins) vs. crater diameter (Db, for the next largest ring) to multi-ring basins. Based on the 17 lunar peak-ring basins documented by Wood and Head (1976), the best-fit linear relationship has a correlation coefficient of 0.97, but substantially underestimates the diameters of the ridge ring in multi-ring basins. If multi-ring basins are considered separately from peak-ring basins, two equally good fits can be made to both sets of data (Fig. 7). The

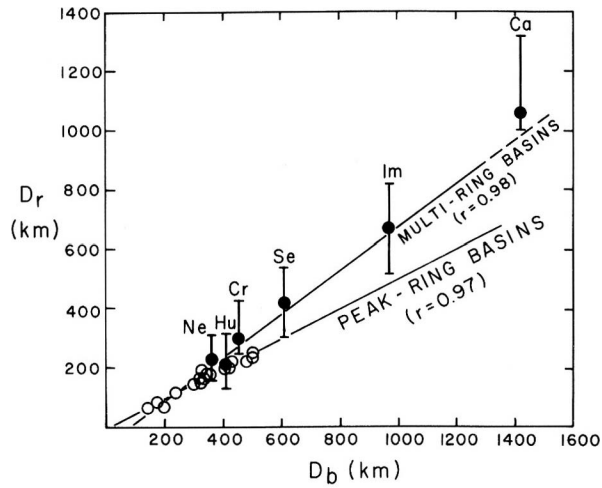

Fig. 7. Comparison of peak-ring and ridge-ring diameters (Dr; vertical axis) with crater or basin rim diameter (Db). Peak rings occur at smaller diameters than ridge rings in multi-ring basins, suggesting two distributions. Vertical line shown for multi-ring basins (name abbreviated above the line) indicates range of location of ridges.

slope of the line for peak-ring basins (0.51) is only slightly less than that found by Head (1978) for peak-ring basins on the Moon, Mars and Mercury. The relatively steeper slope of the regression line for multi-ring basins is consistent with their generally higher ridge-ring/crater rim ratios. A statistical basis for separating the two(?) ring distributions must await further studies detailing the variation in peak-ring location. It is possible that using the outer or inner edges of the peak ring may substantially change the best fit lines used here.

On the basis of ring geometry alone, therefore, ridge rings do not mark the predicted location of buried peak rings. This discrepancy in ring locations could result from: 1) peak rings forming at greater diameters in multi-ring basins as opposed to smaller basins and craters; 2) modification-stage effects during multi-ring basin formation which may act to retain the rim crest in its original position or move it inward; or 3) ridges forming only in near surface units, and having no relationship to the underlying structure. Although both basement influence and bending-stress solutions are consistent with the basin-related setting, the consistent ratio of ridge ring to basin rim would be fortuitous in light of the variations in load experienced by the mare-filled basins.

Several photogeologic observations support the first two hypotheses. According to Head (1977), the discrepancy in ridge ring/crater rim ratios may be due to the decreased role of terracing in the second ring of multi-ring basins, or to megaterrace formation outside the rim crest which acts to shift the rim crest inward. Both processes could explain the relatively larger ridge ring/crater rim ratios for multi-ring basins. In Mare Imbrium, isolated highland peaks protrude through the mare at a slightly larger diameter than the ridge systems, suggesting

the influence of a buried peak ring. In several smaller craters on the moon (e.g., Letronne, the Flamsteed ring, Reiner R) the rim is defined both on the basis of ridges and isolated peaks of an original rim. In addition, mare ridges that deviate into the highlands are characterized by scarps and highland sculpture that suggests the influence of structure beneath the mare.

As shown in Fig. 7, the ridge ring of the Caloris basin lies close to the regression line for lunar multi-ring basins and their associated ridge systems. Despite the different tectonic history implied by the fracturing (and uplift?) of the central Caloris basin, this correlation provides further support for basin-control of the location of the ridge system. This result is also consistent with the conclusions of Wood and Head (1976) and Head (1978), who found no planet-specific variations between peak ring diameter and crater diameters.

Ridge density in azimuth

As shown in the histograms of number of ridges per azimuthal zone (Fig. 8), ridge systems of Caloris have a bimodal distribution resulting from relatively few ridges in the eastern sector. This region of relatively few ridges coincides with the area noted by Strom *et al.* (1975) where the rim of the Caloris basin is poorly developed. The lack of compressional stress in this sector could result from the absence of lateral confinement during subsidence of the basin.

Lunar basins, however, are either nonmodal (as in Crisium), or tend to approach a unimodal distribution with the greatest number of ridges in the eastern sectors. Even within the corresponding sectors of the coverage of Caloris, the decrease in the number of ridges in the northern and southern sectors is evident, but this tendency is even more pronounced if the coverage is increased to show the north and south sectors of the lunar basins (Fig. 8).

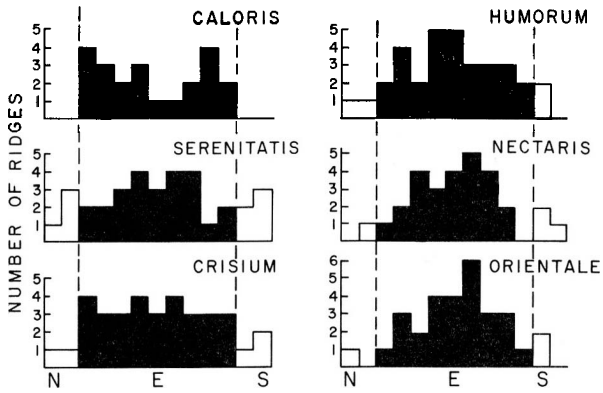

Fig. 8. Histograms showing the number of ridges per azimuth for Caloris and lunar multi-ring basins (represented in 15° bins). Vertical dashed line and filled-in portion of the histograms indicates the extent of Mariner 10 images of Caloris. As a result of deviations into neighboring highlands, relatively few ridges are present in the northern and southern sectors of lunar basins.

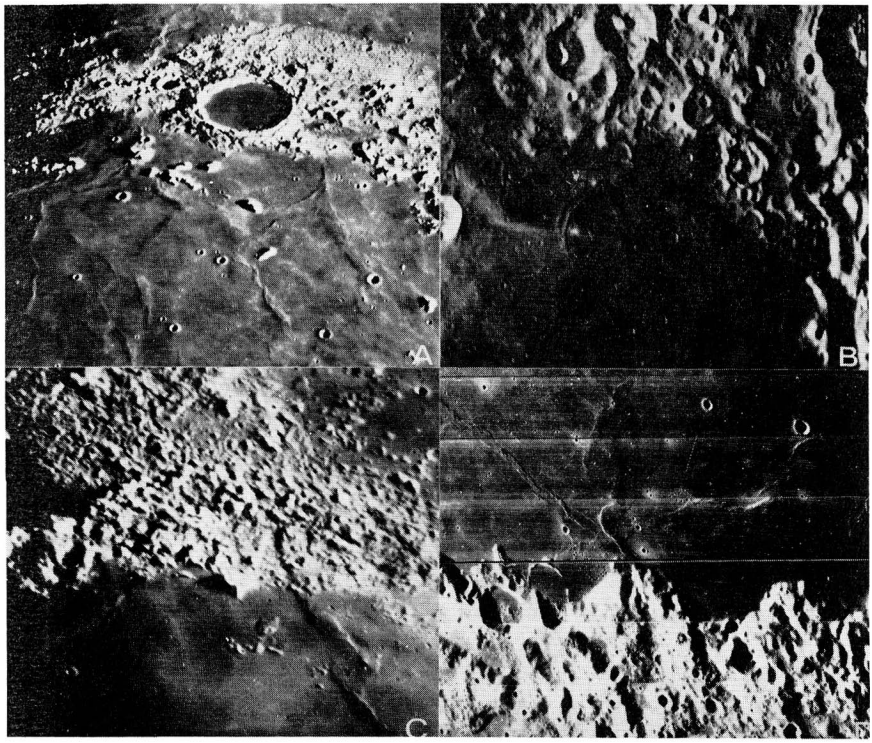

Fig. 9. Deviations of mare ridges into highlands bordering the northern edge of Imbrium (A), Nectaris (B), Serenitatis (C), and the southern edge of Crisium (D). Note the absence of a well-defined circumferential ridge system in the northern sectors of Imbrium, Nectaris and Serenitatis.

For reasons stated above, we believe that the low number of ridges in the northern and southern sectors of lunar basins is not an artifact of E-W lighting, but results from a combination of structural enhancement of N-S trending ridges that continue as highland lineaments (Fig. 9), and a lack of development of circumferential ridges in the northern and southern sectors. Stratigraphically, it is impossible to tell whether the highland scarps are older, reactivated structures, or were formed at the same time as the mare ridges themselves. Assuming a homogeneous tectonic response across the mare-highland contact, the ridges that continue into the highlands could be due to global stress combining with basin-induced hoop stress enhancing the N-S trends. However, since the observed ridge patterns are not truly radial to the basins, and their extensions as highland scarps and lineaments occur outside the range of significant load-induced compression (Solomon and Head, 1980), we believe that the contribution of basin-induced hoop stress was relatively minor compared to that of global compression localized by pre-existing fractures.

The lack of well-defined circumferential ridges and topographic benches in the northern and southern sectors of several lunar basins seems to contradict evi-

dence presented above for control by pre-existing basin structure. Presumably, any impact-related ring structure would tend towards circular symmetry, so there is no *a priori* reason to expect a lack of ridges. Consequently, it is most likely that global stress dominated in these sectors and resulted in reactivation of old fracture trends.

CONCLUSIONS

Comparison of the ridge system of Caloris with those of lunar multi-ring basins indicates that the early evolution of Caloris was similar to that of lunar mascon basins. The morphology of ridges within Caloris compares favorably with lunar ridges when viewed on similar resolution earth-based lunar photographs. Ridges in Caloris occur from 1000 to 1320 km diameter range, and are situated within the boundary delineated by topographic benches in the northeastern and southeastern parts of the basin. The orientation of Caloris ridges is more dominantly concentric than ridge orientations in lunar basins, which supports an origin for Caloris ridges after the major effects of global contraction and/or despinning. In addition, the location of the most prominent ridge-ring in Caloris is similar to that of lunar basins, although the peak ring may not directly underlie the ridge ring. In contrast to lunar basins, however, ridges in Caloris are more abundant than in lunar basins, resulting from either material property differences, or the possibility that we are seeing an early stage of basin settling not covered by later mare basalts as on the moon.

In lunar basins, the effect of global east-west compression is most evident in the northern and southern sectors of the basins, where ridges are continuous with highland scarps and lineaments. Here, global-scale compression dominated over that induced by basin subsidence, resulting in the reactivation of pre-mare fractures. In order to account for the enhancement of the circumferential trends in the eastern and western sectors of lunar basins, and the lack of these trends in the northern and southern sectors, we believe that a significant component of global-scale compression must have been present at the time of ridge formation. Unfortunately, images of the key northern and southern sectors of Caloris do not exist, but based on the distribution and orientation of ridges in the available one-third of the basin, our results provide further evidence that the ridge systems of Caloris developed primarily by basin-induced stress.

The difference in tectonic style between Caloris and lunar basins is also expressed outside the basin rim. In lunar basins, circumferential graben most likely resulted from subsidence of the basin interior in response to basalt loading and thus producing extensional stress surrounding the basins (Solomon and Head, 1980). The lack of graben surrounding Caloris has been attributed to the overriding effect of global compression acting to inhibit extensional faulting (Cordell and Strom, 1977). However, it is also possible that Caloris did not receive the same magnitude of excess mass (volcanic fill?) as lunar basins (Melosh and Dzurisin, 1978b) or that the fill was not basin-wide in extent. The bulk of Caloris fill may

have been confined within the zone represented by the most prominent ridge systems, centered around the second ring (McKinnon, 1979). Thus, the radial and concentric fractures of the central Caloris basin could have formed during the latest stages of subsidence, by extensional stress across the central basin created by subsidence of an annular load. Because of later filling, it is unknown whether lunar basins went through a similar history of loading and tectonic responses.

Acknowledgments—We thank J. W. Head, S. C. Solomon, J. L. Whitford-Stark and C. A. Wood for their helpful reviews. Mariner 10 images used in this study were provided by NSSDC. This research was supported by the National Air and Space Museum, Smithsonian Institution, and by NASA Grant NSG-7188.

REFERENCES

Brennan W. J. (1976) Multiple ring structures and the problem of correlation between lunar basins. *Proc. Lunar Sci. Conf. 7th,* p. 2833–2843.

Cordell B. M. and Strom R. G. (1977) Global tectonics of Mercury and the Moon. *Phys. Earth Planet. Inter.* **15,** 146–155.

Dzurisin D. (1978) The tectonic and volcanic history of Mercury as inferred from studies of scarps, ridges, troughs, and other lineaments. *J. Geophys. Res.* **83,** 4883–4906.

Elston W. E., Laughlin A. W., and Brower J. A. (1971) Lunar nearside tectonic patterns from Orbiter IV photographs. *J. Geophys. Res.* **76,** 5670–5674.

Fagin S. W., Worrall D. M., and Muehlberger W. R. (1978) Lunar mare ridge orientations: Implications for lunar tectonic models. *Proc. Lunar Planet. Sci. Conf. 9th,* p. 3473–3479.

Hapke B., Danielson G. E. Jr., Klaasen K., and Wilson L. (1975) Photometric observations of Mercury from Mariner 10. *J. Geophys. Res.* **80,** 2431–2443.

Hartmann W. K. and Wood C. A. (1971) Moon: Origin and evolution of multi-ring basins. *The Moon* **3,** 3–78.

Head J. W. (1977) Origin of outer rings in lunar multi-ringed basins: Evidence from morphology and ring spacing. In *Impact and Explosion Cratering* (D. J. Roddy, R. O. Pepin, and R. B. Merrill, eds.), p. 563–573. Pergamon, N.Y.

Head, J. W. (1978) Origin of central peaks and peak rings: Evidence from peak-ring basins on Moon, Mars, and Mercury (abstract). In *Lunar and Planetary Science IX,* p. 485–487. Lunar and Planetary Institute, Houston.

Kuiper G. P., Whitaker E. A., Strom R. G., Fountain J. W., and Larson S. M. (1967) Consolidated lunar atlas, Supp. nos. 3 and 4 to USAF photographic lunar atlas. *Contr. Lunar and Planetary Lab., Univ. Ariz.* **4,** 24 pp. 226 photographs.

Lucchitta B. K. (1976) Mare ridges and related highland scarps—Result of vertical tectonism? *Proc. Lunar Sci. Conf. 7th,* p. 2761–2782.

Lucchitta B. K. (1977) Topography, structure, and mare ridges in southern Mare Imbrium and northern Oceanus Procellarum. *Proc. Lunar Sci. Conf. 8th,* p. 2691–2703.

Malin M. C. (1978) Surfaces of Mercury and the moon: Effects of resolution and lighting conditions on the discrimination of volcanic features. *Proc. Lunar Planet. Sci. Conf. 9th,* p. 3395–3409.

Maxwell T. A. (1978) Origin of multi-ring basin ridge systems: An upper limit to elastic deformation based on a finite-element model. *Proc. Lunar Planet. Sci. Conf. 9th,* p. 3541–3559.

Maxwell T. A., El-Baz F., and Ward S. H. (1975) Distribution, morphology and origin of ridges and arches in Mare Serenitatis. *Bull. Geol. Soc. Amer.* **86,** 1273–1278.

Maxwell T. A. and Phillips R. J. (1978) Stratigraphic correlation of the radar-detected subsurface interface in Mare Crisium. *Geophys. Res. Lett.* **5,** 811–814.

McKinnon W. B. (1979) Caloris: Ring load on an elastic lithosphere (abstract). *EOS (Trans. Amer. Geophys. Union)* **60,** 871.

Melosh H. J. and Dzurisin D. (1978a) Mercurian global tectonics: A consequence of tidal despinning? *Icarus* **35,** 227–236.

Melosh H. J. and Dzurisin D. (1978b) Tectonic implications for the gravity structure of Caloris Basin, Mercury. *Icarus* **33,** 141–144.

Muehlberger W. R. (1974) Structural history of southeastern Mare Serenitatis and adjacent highlands. *Proc. Lunar Sci. Conf. 5th,* p. 101–110.

Peeples W. J., Sill W. R., May T. W., Ward S. H., Phillips R. J., Jordan R. L., Abbott E. A., and Killpack T. J. (1978) Orbital radar evidence for lunar subsurface layering in Mare Serenitatis and Crisium. *J. Geophys. Res.* **83,** 3459–3468.

Phillips R. J., Conel J. E., Abbott E. A., Sjogren W. L., and Morton J. B. (1972) Mascons: Progress toward a unique solution for mass distribution. *J. Geophys. Res.* **77,** 7106–7114.

Solomon S. C. (1977) The relationship between crustal tectonics and internal evolution in the Moon and Mercury. *Phys. Earth Planet. Inter.* **15,** 135–145.

Solomon S. C. and Head J. W. (1980) Lunar mascon basins: Lava filling, tectonics, and evolution of the lithosphere. *Rev. Geophys. Space Phys.* **18,** 107–141.

Strom R. G. (1964) Analysis of lunar lineaments, I: Tectonic maps of the Moon. *Contr. Lunar and Planetary Lab, Univ. Ariz.* **2,** 205–216.

Strom R. G. (1979) Mercury: A post-Mariner 10 assessment. *Space Sci. Rev.* **24,** 3–70.

Strom R. G., Trask N. J., and Guest J. E. (1975) Tectonism and volcanism on Mercury. *J. Geophys. Res.* **80,** 2478–2507.

U.S.G.S. (1979) Shaded relief map of the Caloris Planitia area of Mercury. U.S. Geol. Survey Misc. Geol. Inv. Map I-1172, 1:5,000,000.

Wilhelms D. E. and McCauley J. F. (1971) Geologic map of the near side of the Moon. U.S. Geol. Survey Misc. Geol. Inv. Map I-703, 1:5,000,000.

Wood C. A. and Head J. W. (1976) Comparison of impact basins on Mercury, Mars and the Moon. *Proc. Lunar Sci. Conf. 7th,* p. 3629–3651.

Wood C. A., Head J. W., and Cintala M. J. (1977) Crater degradation on Mercury and the Moon: Clues to surface evolution. *Proc. Lunar Sci. Conf. 7th,* p. 3503–3520.